Precise $\sin^2 2\theta_{13}$ measurement by the Daya Bay reactor neutrino experiment.

M. Gonchar on behalf of Daya Bay Collaboration*
Joint Institute for Nuclear Research, Dubna - 141980, Russia

The Daya Bay reactor neutrino experiment was designed for the precise measurement of the $\sin^2 2\theta_{13}$ neutrino mixing angle. The angle is essential for the understanding of the neutrino oscillations. It is also important for observing CP violation in leptonic sector.

The experiment is located near one of the most powerful nuclear stations — Daya Bay (Shenzhen, China) which produces 17.4 GW of thermal power. To measure the antineutrino disappearance probability 6 identical antineutrino detectors with a total target mass of 120 tons are used. Three detectors are located in two sites near the reactor cores (500 meters on average) to measure the total antineutrino flux and three detectors are located in the far site (1.7 km on average). Two more detectors are to be installed later this year. The experiment's layout along with strong background suppression and accurate detector calibrations provide the goal $\sin^2 2\theta_{13}$ sensitivity of 0.01.

The experiment started taking data on 24 of December, 2011. The first Daya Bay's result indicating non-zero $\sin^2 2\theta_{13}$ at the 5.2σ level was published in March 2012. In May the significance was increased to a 7.7σ level.

The updated Daya Bay's results are presented in this talk.

1. Introduction

The neutrino mixing is described by PMNS mixing matrix, which consists of 4 parameters: three rotation angles $\theta_{12}, \theta_{23}, \theta_{13}$ and CP-violating phase δ_{CP}. While two angles were measured with satisfactory precision (θ_{12} and θ_{23}), the mixing angle θ_{13} had only the upper limit[1] ($\sin^2 2\theta_{13} < 0.15$ at 90% C. L.). The value of δ_{CP} is currently unknown. It can be observed only if θ_{13} is non-zero.

The θ_{13} mixing angle can be observed in electron neutrino oscillations. The survival probability is given by the following equation:

$$P_{ee} = 1 - \sin^2 2\theta_{13} \sin^2 \Delta_{31} - \cos^4 \theta_{13} \sin^2 2\theta_{12} \sin^2 \Delta_{21} \quad (1)$$

$$\Delta_{jk} = 1267 \cdot \frac{\Delta m^2_{jk}}{\mathrm{eV}^2} \frac{L}{\mathrm{km}} \frac{\mathrm{MeV}}{E}, \quad (2)$$

where Δm^2_{31} and Δm^2_{21} are the differences of squared neutrino masses.

The usual way of measuring θ_{13} is the observation of the electron antineutrino disappearance in reactor-based experiments. In order to minimize flux related uncertainties several detectors are used. The near detector measures the antineutrino flux, not affected by oscillations and the far detector measures the oscillated flux.

Electron antineutrino is detected via inverse β-decay (IBD) reaction:

$$\bar{\nu}_e + p \longrightarrow e^+ + n \quad (3)$$

The positron almost immediately releases its energy and annihilates with electron (prompt signal). The prompt signal visible energy is between 1.022 MeV and 10 MeV. The neutron is thermalized in average of 28μs and is captured by a Gd nucleus which then emits several gammas of summary energy of 8 MeV (delayed signal).

In 2011-2012 several experiments (KamLAND[2], MINOS[3], T2K[4] and Double CHOOZ[5]) claimed to see non-zero θ_{13} value. In March 2012 the first evidence of non-zero θ_{13} with confidence level above 5σ was stated by the Daya Bay[6] experiment.

*Electronic address: maxim.mg.gonchar@gmail.com

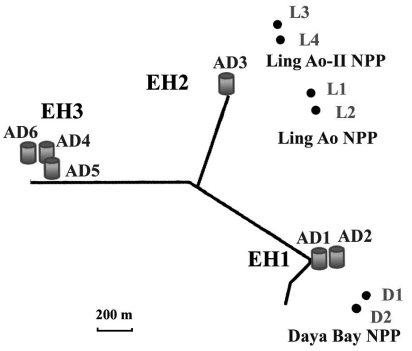

FIG. 1: Daya Bay experiment layout.

	Overburden	D. B.	L. A.	L. A. II
EH1	280	360	860	1310
EH2	300	1250	480	530
EH3	880	1910	1540	1550

TABLE I: Approximate overburden (m. w. e.) and distances between detectors and reactor cores (m).

2. Experiment layout

The Daya Bay experiment is located near one of the most powerful nuclear power stations — Daya Bay, near Shenzhen, China. NPP consists of six reactor cores (see Fig. 1) located in three sites: Daya Bay (D1, D2), Ling Ao (L1, L2), Ling Ao II (L3, L4). The maximal NPP thermal power is 17.4 GW_{th} (2.9 GW_{th} for each core).

The detailed experiment description can be found in [6], [7] and [8].

Six (eight planned) identical detectors are installed in three experimental sites: two detectors (EH1) in average 360 m from Daya Bay reactor core, one detector (EH2) in average 500 m from Ling Ao I&II cores and three detectors (EH3) in place with maximum oscillation probability in average 1650 m from all reactor cores. The experimental sites are located underground and connected by a single tunnel. The overburden of the experimental sites as well as the distances between detectors and reactors are listed in table I. The second detector at EH2 and the fourth detector at EH3 are to be installed on summer 2012.

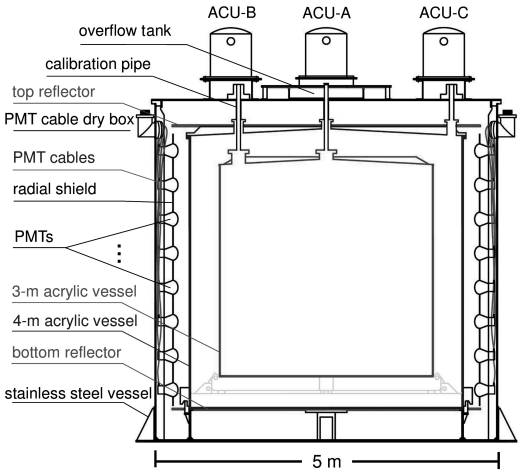

FIG. 2: The antineutrino detector scheme.

The antineutrino detector (AD) utilizes the three-zone scintillator detector structure (see Fig. 2). It consists of three concentric cylindric volumes. The innermost volume is the target: 3.1 m diameter and height acrylic vessel (IAV). It holds 20 t of liquid scintillator, doped by 0.1% of gadolinium. IAV is located inside the outer acrylic vessel (OAV) filled with 21 t of undoped liquid scintillator used to catch gammas escaping IAV. The middle volume is called "gamma-catcher". The OAV is 4 m diameter and height. It is located in stainless steel vessel (SSV) of 5 m diameter and height. The outermost volume is filled with 37 t of mineral oil (MO) used as shield against the radiation. The comparison of two near ADs and their performance is presented in [8].

192 8-inch photomultiplier tubes (PMT) are installed in 24 columns and 8 rings on the inner surface of SSV to collect the light, emitted by scintillation of the LS. The PMTs are recessed inside a black acrylic cylindrical shield, located at the equator of PMT bulb used to minimize the light reflection from the walls. Two 4.5 m diameter reflective discs are installed on top and bottom of the OAV. Their purpose is to increase the light collection and improve the uniformity of energy response. Six 2-inch PMTs are installed on top and bot-

tom of the AD to monitor LS and GdLS refraction index.

There are three automated calibration units (ACU) mounted on top of the SSV. Two units are connected to the IAV: ACU-A can be lowered into the GdLS along the IAV central axis, ACU-B can be lowered near the IAV edge. ACU-C is connected to the OAV and can be lowered into the LS. Each ACU contains a LED light source and two sealed capsules with radioactive isotopes.

Several ADs (two at the DB site, one at the LA site and three at the Far site) are located in the water pool, filled with purified and deoxidized water (1200 t and 1950 t for near and far sites respectively) and used as Cerenkov detector. Each AD is shielded by >2.5 meters of high purity water. Water pool is optically divided in two parts: inner and outer water shield (IWS and OWS), each acting as separate muon detector. Water shields are covered with PMTs.

RPC[9] modules are mounted to cover the water pool. 2 x 2 m RPC modules are installed in zig-zag mode overlapping each other to increase the spatial resolution. Each RPC module have 4 layers of RPCs.

Each ACU is equipped with several radiation sources which can be deployed separately. LED is used to calibrate the PMT timing, single photon response and relative quantum efficiency. Gammas of total energy of 2.5 MeV emitted by ^{60}Co are used to calibrate the energy scale. ^{68}Ge generates pairs of 511 KeV gammas and used to energy calibration around the threshold. ^{241}Am^{13}C is the source emitting neutrons with frequency of 0.5 Hz is used to analyse the neutron capture time and H/Gd capture ratio.

3. Background rates and efficiencies

The following types of the backgrounds are taken into account: the accidental coincidence of two random triggers, β-n decaying ^{8}He/^{9}Li isotopes, fast neutrons, ^{13}C$(\alpha, n)^{16}$O interactions and background signals induced by the Am-C radioactive source from ACU.

An accidental event happens when two triggers caused by essential radioactivity and/or neutron interactions are in the detection window. It's rate is determined by counting prompt-like and delayed-like signals in separate and calculating the probability of their coincidence in the same time window.

The ACU related background is caused by the Am-C generated neutrons. They can produce gammas via the inelastic scattering in SSV and after the neutron capture on Fe/Cr/Mn/Ni. Both gammas can enter the target region mimicking the prompt and the delayed signal. The ACU background is estimated using the MC simulation.

The α particle emitted from the U/Th decay chain, can interact with ^{13}C causing (α, n) reaction, which produces ^{16}O nucleus, neutron (delayed signal) and 2.2 MeV gammas (prompt signal). The ^{13}C$(\alpha, n)^{16}$O background rate is determined via MC, after estimating amount of ^{238}U, ^{232}Th, ^{227}Ac and ^{210}Po in the GdLS based on their cascade decays.

Two other background sources are related to the cosmogenic muons. The long-living isotopes ^{8}He/^{9}Li can survive the trigger time. They are produced in muon interactions inside the AD. Decaying they emit both the neutron and the β-particle which mimic delayed and prompt signals. The ^{8}He/^{9}Li was determined by fitting the time since the last muon assuming the known decay time of the isotopes.

Fast neutrons are also produced via the muon interaction. They produce the prompt signal by recoiling free protons in the AD, the delayed signal is the fast neutron capture itself. The fast neutron rate is determined by counting the events with prompt energy >12 MeV and extrapolating their spectrum to the lower energy region.

The uncorrelated detection inefficiency is formed by the muon detection inefficiency and the multiplicity selection inefficiency. The muon detection inefficiency is calculated by integrating the vetoed time of each muon with temporal overlaps taken into account. The multiplicity selection inefficiency is determined by calculating the probability of a ran-

	Near sites			Far site		
	AD1	AD2	AD3	AD4	AD5	AD6
IBD candidates	69121	69714	66473	9788	9669	9452
DAQ live time (days)	127.5470		127.3763		126.2646	
Muon veto time (days)	22.5656	22.9901	18.14.26	2.3619	2.3638	2.4040
Efficiency	0.8015	0.7986	0.8364	0.9555	0.9552	0.9547
Accidentals (/day)	9.73±0.10	9.61±0.10	7.55±0.08	3.05±0.04	3.04±0.04	2.93 ± 0.03
Fast neutrons (/day)	0.77±0.24	0.77±0.24	0.58±0.33		0.05±0.02	
^{9}Li/^{8}He (/AD/day)	2.9±1.5		2.0±1.1		0.22±0.12	
AmC (/AD/day)	0.2±0.2				0.2±0.2	
^{13}C^{16}O (/day)	0.08±0.04	0.07±0.04	0.05±0.03		0.04±0.02	
IBD rate (/day)	662.47±3.00	670.87±3.01	613.53±2.69	77.57±0.85	76.62±0.85	74.97±0.84

TABLE II: Signal and background summary.

dom trigger to occur in a time window with the IBD event. The average of the values of efficiencies are given in the table III.

The additional correction to the number of IBD events are applied due to geometrical effects: the "spill-in" correction takes into account Gd capture of neutrons from the IBD interactions outside the target region, the "spill-out" correction takes into account IBD neutrons leaving the target region. The "spill-in" correction is calculated based on the MC simulation. The "spill-out" correction is included into the Gd capture ratio and studied using the Am-C source and the MC.

The instrumental background caused by spontaneous light emission by PMTs ("flashers") is effectively rejected by the cuts in which the clustering of detector response is analyzed.

4. Event selection

The following trigger criteria for the ADs are used: number of hit PMTs>45 and total visible energy>0.4 MeV. Trigger time and charge are saved for each PMT. The energy is reconstructed based on the total number of collected pe with the factor of ∼163. The factor is determined by fitting 2.506 MeV ^{60}Co peak. The energy resolution is $(7.5/\sqrt{E(MeV)}+0.9)\%$ for all ADs.

The water pool events are triggered by the NHIT>12 and marked as muon candidates. Muon candidates with energy deposit inside the AD in a time window ±2μs are marked as AD muons for E>20 MeV and showering muons for E>2.5 GeV.

	Eff.	Corr.	Uncorr.
Target protons		0.47%	0.03%
Flasher cut	99.98%	0.010%	0.01%
Delayed E cut	90.9%	0.6%	0.12%
Prompt E cut	99.88%	0.10%	0.01%
Multiplicity cut		0.02%	<0.01%
Capture time cut	98.6%	0.12%	0.01%
Gd capture ratio	83.8%	0.8%	<0.1%
Spill-in	105.0%	1.5%	0.02%
Livetime	100.0%	0.002%	<0.01%
Combined	78.8%	1.9%	0.2%

TABLE III: Summary of the detector efficiencies and uncertainties.

The IBD events were selected using the following criteria: prompt signal with visible energy between 0.7 and 12 MeV, delayed signal with visible energy between 6 and 12 MeV, time distance between signals is required to be between 1 and 200 μs. No other signal with energy higher than 0.7 MeV is required in 200 μs before the prompt or after the delayed signal. The are should be detected no WS muons in in a time window of 600 μs before the delayed signal, no AD muons in a time window of 1000 μs and no showering muons in a second before the delayed signal.

5. Analysis

In order to minimize the systematic uncertainties only the period when all 6 detectors were active is used. The first analysis pub-

Correlated		Uncorrelated	
Energy/fission	0.2%	Power	0.5%
IBD/fission	3%	Fission fraction	0.6%
		Spent fuel	0.3%
Combined	3%	Combined	0.8%

TABLE IV: Summary of the reactor uncertainties.

lished in [6] is based on data acquired in the period from 24 December 2011 to 17 February 2012. The improved analysis is based on data from 24 December 2011 to 11 of May 2012. The number of collected IBD candidates as well as data acquisition time and expected signal and background rates are presented in the table II.

The near to far ratio is calculated by weighting the data from near sites assuming no oscillations. The weights are determined based on thermal power of the reactors and the baselines. The deficit in the far site rate was observed:

$$R = 0.944 \pm 0.007 \text{ (stat)} \ \pm 0.003 \text{ (syst)} \quad (4)$$

The χ^2 rate-only analysis is used to determine the value of $\sin^2 2\theta_{13}$. The analysis was independent on reactor flux models. The systematic errors were taken into account by introducing the pull-terms:

$$\chi^2 = \sum_{d=1}^{6} \frac{\left[M_d - T_d(1+\varepsilon\sum_r \omega_r^d \alpha_r + \varepsilon_d) + \eta_d\right]^2}{M_d + B_d} + \sum_r \frac{\alpha_r^2}{\sigma_r^2} + \sum_{d=1}^{6}\left(\frac{\varepsilon^2}{\sigma_d^2} + \frac{\eta_d^2}{\sigma_B^2}\right), \quad (5)$$

where M_d is the number of IBD candidates in the d-th AD with backgrounds subtracted, T_d is the number of expected IBD events, ε is the global normalization factor, ω_r^d is the fraction of the IBD events seen in the d-th detector from the r-th reactor, B_d is the background in the d-th detector. σ_r, σ_d are the uncorrelated reactor and detector uncertainties and σ_B is the background uncertainty. All systematic uncertainties are listed in tables III and IV. Only uncorrelated uncertainties are included into the analysis. The global normalization is determined by the fit to data.

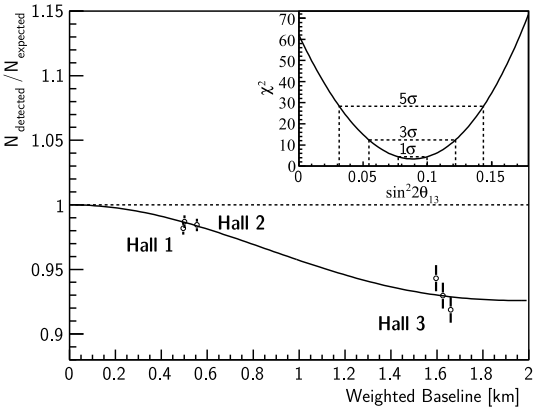

FIG. 3: The ratio of measured number of events to the expected assuming no oscillation hypothesis in each AD. Error bar is the individual uncorrelated uncertainty of the AD. The χ^2 vs $\sin^2 2\theta_{13}$ is shown in the corner.

The best fit value is:

$$\sin^2 2\theta_{13} = 0.089 \pm 0.010 \text{ (stat)} \pm 0.005 \text{ (syst)}, \quad (6)$$

with χ^2/NDF =3.4/4. The no-oscillation hypothesis is excluded at 7.7σ level.

The ratio of measured number of events vs the no oscillation hypothesis is shown on the Fig. 3. The clear 5.6% deficit can be seen. The χ^2 vs $\sin^2 2\theta_{13}$ is shown in the corner. The ratio of the measured prompt energy spectrum of the far hall to the prediction from the near halls is shown on the Fig. 4.

6. Acknowledgments

The Daya Bay experiment is supported in part by the Ministry of Science and Technology of China, the United States Department of Energy, the Chinese Academy of Sciences, the National Natural Science Foundation of China, the Guangdong provincial government, the Shenzhen municipal government, the China Guangdong Nuclear Power Group, Shanghai Laboratory for Particle Physics and Cosmology, the Research Grants Council of the Hong Kong Special Administrative Region of China, University Development Fund of The University of Hong Kong, the MOE program for Research of Excellence at National

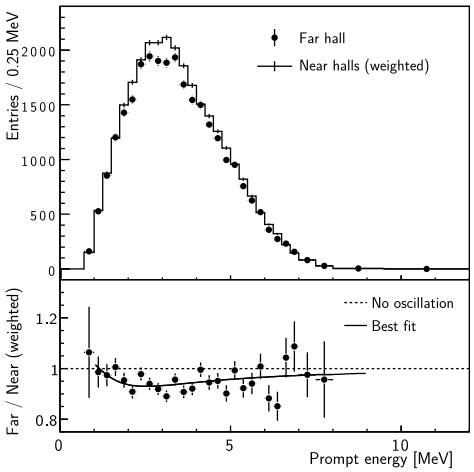

FIG. 4: Top: The measured prompt energy spectrum at the far hall compared to the no oscillation prediction based on weighted measurement of the near halls. Spectra are background subtracted. Bottom: the ratio of the spectra. Smooth curve is the ratio expected for the $\sin^2 2\theta_{13} = 0.089$, obtained from the rate-only analysis.

Taiwan University, National Chiao-Tung University, and NSC fund support from Taiwan, the U.S. National Science Foundation, the Alfred P. Sloan Foundation, the Ministry of Education, Youth and Sports of the Czech Republic, the Czech Science Foundation, and the Joint Institute of Nuclear Research in Dubna, Russia. We thank Yellow River Engineering Consulting Co., Ltd. and China railway 15th Bureau Group Co., Ltd. for building the underground laboratory. We are grateful for the ongoing cooperation from the China Guangdong Nuclear Power Group and China Light & Power Company.

References

[1] M. Apollonio *et al.* [CHOOZ Collaboration], Phys. Lett. B **466** (1999) 415 [hep-ex/9907037].

[2] G. L. Fogli, E. Lisi, A. Marrone, A. Palazzo and A. M. Rotunno, Phys. Rev. D **84** (2011) 053007 [arXiv:1106.6028 [hep-ph]].

[3] P. Adamson *et al.* [MINOS Collaboration], Phys. Rev. Lett. **107** (2011) 181802 [arXiv:1108.0015 [hep-ex]].

[4] K. Abe *et al.* [T2K Collaboration], Phys. Rev. Lett. **107** (2011) 041801 [arXiv:1106.2822 [hep-ex]].

[5] Y. Abe *et al.* [DOUBLE-CHOOZ Collaboration], Phys. Rev. Lett. **108** (2012) 131801 [arXiv:1112.6353 [hep-ex]].

[6] F. P. An *et al.* [DAYA-BAY Collaboration], Phys. Rev. Lett. **108** (2012) 171803 [arXiv:1203.1669 [hep-ex]].

[7] X. Guo *et al.* [Daya-Bay Collaboration], hep-ex/0701029.

[8] F. P. An, *et al.* [Daya Bay Collaboration], Nucl. Instrum. Meth. A **685** (2012) 78 [arXiv:1202.6181 [physics.ins-det]].

[9] J. -L. Xu, M. -Y. Guan, C. -G. Yang, Y. -F. Wang, J. -W. Zhang, C. -G. Lu, K. McDonald and R. Hackenburg *et al.*, Chin. Phys. C **35** (2011) 844.